Clay minerals in delta deposits and organic preservation potential on Mars

BETHANY L. EHLMANN[1]*, JOHN F. MUSTARD[1], CALEB I. FASSETT[1], SAMUEL C. SCHON[1], JAMES W. HEAD III[1], DAVID J. DES MARAIS[2], JOHN A. GRANT[3] AND SCOTT L. MURCHIE[4]

[1]Department of Geological Sciences, Brown University, Providence, Rhode Island 02912, USA
[2]NASA Ames Research Center, Mountain View, California 94035, USA
[3]Center for Earth and Planetary Studies, National Air and Space Museum, Smithsonian Institution, Washington, DC 20013, USA
[4]Applied Physics Laboratory, Johns Hopkins University, Laurel, Maryland 20723, USA
*e-mail: bethany_ehlmann@brown.edu

Published online: 18 May 2008; doi:10.1038/ngeo207

Clay-rich sedimentary deposits are often sites of organic matter preservation[1,2], and have therefore been sought in Mars exploration[3]. However, regional deposits of hydrous minerals, including phyllosilicates and sulphates[4,5], are not typically associated with valley networks and layered sediments that provide geomorphic evidence of surface water transport on early Mars[6–8]. The Compact Reconnaissance Imaging Spectrometer for Mars (CRISM)[9] has recently identified phyllosilicates[10] within three lake basins with fans or deltas that indicate sustained sediment deposition: Eberswalde crater[7,11,12], Holden crater[12,13] and Jezero crater[14]. Here we use high-resolution data from the Mars Reconnaissance Orbiter (MRO) to identify clay-rich fluvial–lacustrine sediments within Jezero crater, which has a diameter of 45 km. The crater is an open lake basin on Mars with sedimentary deposits of hydrous minerals sourced from a smectite-rich catchment in the Nili Fossae region. We find that the two deltas and the lowest observed stratigraphic layer within the crater host iron–magnesium smectite clay. Jezero crater holds sediments that record multiple episodes of aqueous activity on early Mars. We suggest that this depositional setting and the smectite mineralogy make these deltaic deposits well suited for the sequestration and preservation of organic material.

MRO-CRISM[9] provides hyperspectral visible-to-near-infrared images at 18 m per pixel, and MRO's High Resolution Imaging Science Experiment (HiRISE)[15] instrument provides images at 0.25 m per pixel. We couple CRISM and HiRISE with Mars Orbiter Laser Altimeter (MOLA) topographic data to investigate the geomorphology and mineralogy of Jezero crater deposits at high resolution. Jezero crater lies within Noachian terrain[16] south of Nili Fossae, which is basaltic and enriched in iron-bearing igneous minerals such as olivine and low-calcium pyroxene[17–19]. Previous analysis of the Jezero crater catchment and deltaic deposits indicates that it hosted a long-lived (estimated at least $\sim 10^3$ yr) crater lake[14]. The minimum volume of Jezero lake required to sustain a stream in its outlet valley is approximately 250 km^3, larger than present-day Lake Tahoe on Earth ($\sim$160 km^3). A $\sim$15,000 km^2 catchment sustained Jezero crater lake during the late Noachian or early Hesperian and it drained through an outlet valley to the east[14].

Data from the Mars Express Observatoire pour la Minéralogie, l'Eau, les Glaces et l'Activité (OMEGA)[4] show that the watershed associated with Jezero crater contains extensive outcrops of iron–magnesium smectite-bearing rock exposed along incised valleys[5,20] (Fig. 1). MOLA point-shot elevation profiles of the main valleys and tributaries show that at least 58 km^3 of sediment was eroded and transported from the clay-rich section of the Noachian plateau sequence by two valleys draining into Jezero crater, indicating that these clay minerals may comprise a significant fraction of the sediments within Jezero.

Delta deposits are found at the mouth of the fluvial valleys which enter the crater from the west and north[14] (Fig. 1c). HiRISE shows at least two distinct units within the well-preserved western delta: (i) darker capping material that lacks observable bedding structure and (ii) layered bright material with arcuate bed forms (Fig. 2). Unit (i) is 5–10 m thick and exists in cross-cutting lobate deposits, which are not texturally homogenous. Some are friable and erode to form debris of a size not resolvable by HiRISE. Other lobes are more competent and shed metre-scale angular boulders from $\sim$5 m cliffs. Unit (ii) is at least 20 m thick and consists of light-toned layered deposits. Metre-scale arcuate bedforms are exposed within this unit in a crater wall (Fig. 2c) and in eroded portions of the delta (Fig. 2e). Stereo viewing of HiRISE image pairs shows that the arcuate structures are often low angle but sometimes form slight ridges when eroded, probably owing to differences in grain size, cementation or composition within the deposits. Unit (ii) (bright layered materials, Fig. 2d) forms slopes beneath unit (i), typical for fine-grained units overlain by more competent material.

Additional units can be mapped elsewhere on the crater floor. Bright materials with polygonal fractures (iii) are overlain by a darker smooth, massive unit (iv) that has a defined boundary in the eastern portion of the crater (Fig. 2a). The thickness of this upper unit (iv) is $<$20 m, and in depressions where (iv) is absent, exposing underlying materials, dark ripples and dunes (v) form an aeolian deposit that intermittently covers the bright unit (iii) (Fig. 2f). The bright unit (iii) drapes the crater wall and extends out into the basin for at least 12 km, the limit of HiRISE and CRISM coverage, and is exposed in windows a few tens of square metres in size, beneath unit (iv) and the sand cover (v).

The mineralogical composition of the crater rim, wall and floor materials can be determined by CRISM visible-to-near-infrared spectral data. The crater is emplaced in pyroxene-bearing rock, indicated by CRISM spectra of exposed materials on the

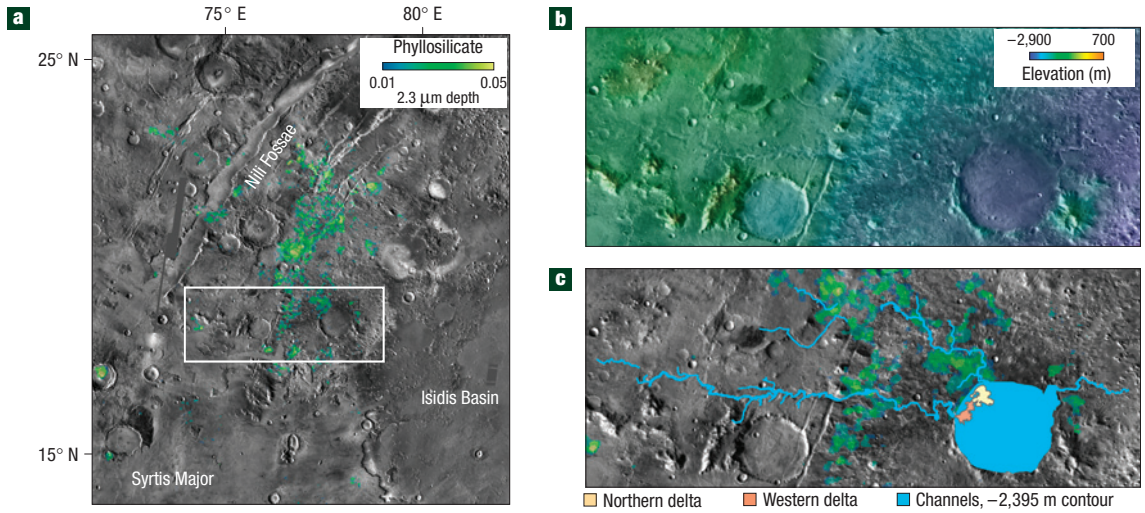

Figure 1 Mineralogy and extent of the Jezero crater watershed. a, Mars Odyssey THEMIS day infrared image with overlain OMEGA phyllosilicate detections, mapped using the D2300 parameter for band depth at 2.3 μm (ref. 10). The white box indicates the location of **b** and **c**. **b**, MOLA colour elevation map of the Jezero crater watershed **c**, Phyllosilicates in the watershed as shown in **a**, with superimposed mapping of the Jezero valley system, the lake at overflow depth and the extent of two deltas within the crater.

southwestern rim (Figs 2b, 3). Modified gaussian model spectral deconvolution[21] shows that the pyroxene is low-calcium pyroxene enriched (60%), as is common for Noachian crustal materials in this region[17]. The uppermost units within the crater, (i) and (iv), have similar spectral properties: relatively low albedo and no diagnostic absorption features (see Supplementary Information, Fig. S1). The aeolian unit (v) has a broad 1 μm absorption and a spectral shape characteristic of fayalitic olivine (Fig. 3). This material is probably sourced from the same regional olivine-bearing sand cover as blankets much of eastern Nili Fossae[10].

Both delta and crater-floor bright units (ii, iii) have absorption features at 1.9 and 2.3 μm characteristic of iron–magnesium smectites (Fig. 3). The 1.9 μm absorption is due to H_2O in the mineral structure[22]. The centre of the ~2.3 μm metal–OH absorption shifts depending on the relative abundance of iron compared with magnesium in the octahedral layer of the phyllosilicate structure[23]. The band position for Jezero crater bright materials is 2.30 μm, indicating a composition intermediate between iron-rich nontronite (band centre 2.285 μm) and magnesium-rich saponite (2.315 μm) (Fig. 3). Additional absorption features atypical of pure smectite spectra may indicate the presence of additional minerals in light-toned sediments. An absorption feature is present near 2.5 μm. Zeolite and carbonate are two mineral classes with this feature, although these cannot be positively identified because neither the 1.4 μm absorption characteristic of zeolite nor the 3.4 μm overtone of the carbonate fundamental are seen in the spectral data. Weak absorptions below 1 μm, for example ~0.5 μm, are probably due to iron oxides or hydroxides. The strong roll-off at wavelengths below 1.5 μm probably reflects the presence of ferrous iron from Fe-smectite clays or olivine, either intimately mixed with or in sands on top of the phyllosilicate-bearing material. The 1.4 μm band, typical of smectites but weak to absent in spectra acquired from within the crater, may be suppressed by this strong electronic absorption. Sedimentary detrital minerals such as quartz and feldspar do not have unique absorptions in the 0.4–4.0 μm spectral region covered by CRISM, so their presence or absence cannot be inferred.

New MRO data corroborate that the Jezero crater lake system was long lived[14], rather than catastrophic. Evidence for an early higher lake level in Jezero crater is provided by unit (iii) sedimentary phyllosilicates draped on the western walls of the crater up to −2,305 m elevation. Following formation of the outlet valley, the lake level dropped to approximately −2,395 m. Smectite-rich sediments of the western delta were deposited in meandering stream courses in a delta plain environment as the delta built outward into the lake. Scroll bars (Fig. 2e), which are characteristic of migrating point-bar sequences[24], and epsilon cross-beds[25] (Fig. 2c) formed during lateral accretion. Distinct lobes observed within the delta reflect channel-switching events. Structures such as these might also be expected in the later stages of Jezero lake as sedimentation compensated for the lowering water level. The present delta is highly eroded, and the steep escarpment at the margin does not reflect its original morphology. Resistant knobs and lobes of the original delta persist away from the main body of the present delta. The fact that the remaining portion of the delta shows characteristic 'bird's-foot' morphology is probably due to resistance to erosion of the more competent upper units. The fracture pattern of the light-toned units within the crater might result from the expansion and contraction of smectite swelling clays in response to changes in hydration.

An upper limit to the amount of sediment delivered by the valley system to the lake can be estimated from a topographic profile of Jezero crater, which is significantly shallower near the inflows (Fig. 4). Typical Martian craters of this size have a depth to diameter ratio of ~1:20 (ref. 26), but for Jezero crater the value is only 1:45. Jezero is ~800 m shallower than a less degraded crater of comparable size (125.75 E, 8.25 N), presumably because of additional sediments filling the basin (Fig. 4). The ~1,000 km^3 volume of fill in Jezero is far more than the 58 km^3 eroded to form the main valleys, consistent with landscape denudation by surface runoff within the watershed rather than erosion by sapping activity restricted to channels. At least the uppermost part of the Jezero crater fill unit is smectite bearing (Fig. 4b).

The Jezero crater lacustrine system is unique among recognized Martian palaeolakes because it eroded a large watershed of

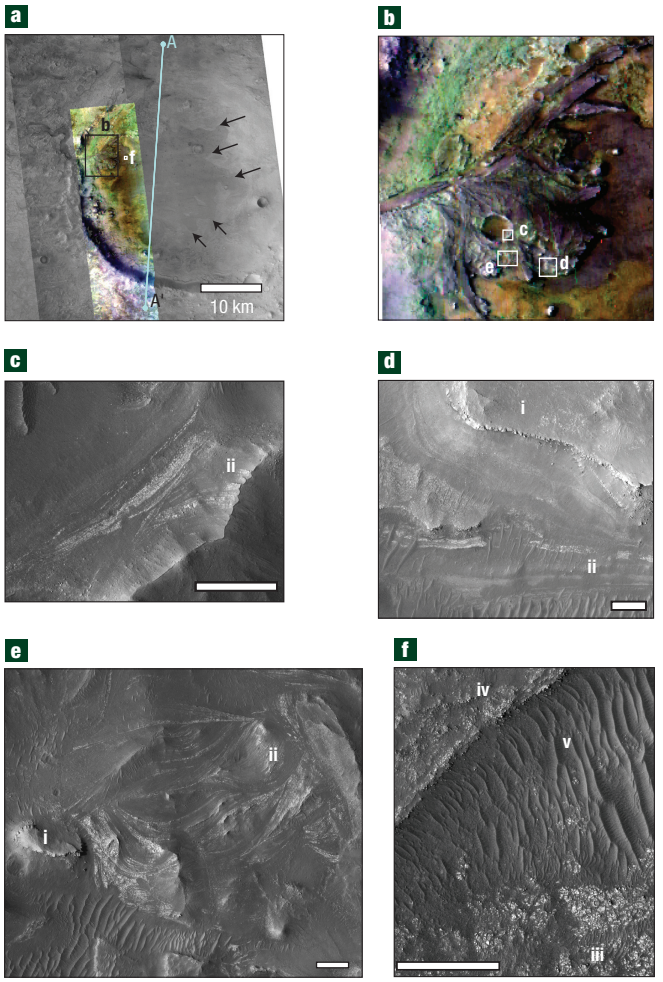

Figure 2 MRO view of Jezero crater. a, Context Imager mosaic (P03_002387_1987_XI_18N282W_070129, P06_003521_1971_XI_17N282W_070427) with overlain false-colour composite CRISM image (MSW00004599; red, 2.38; green, 1.80; blue, 1.15 μm). Phyllosilicate-bearing materials are green, olivine-bearing materials are yellow, low-calcium pyroxene-bearing materials are blue and purple–brown surfaces have no distinct spectral features. Arrows show the margins of the uppermost unit (iv). Profile A–A′ is shown in Fig. 4a. **b**, View of the western fan with high-resolution CRISM image HRL000040FF with colours as in **a**. **c**–**f**, HiRISE (PSP_002387_1985) of epsilon cross-stratification in unit (ii) exposed in the wall of a small crater (**c**), the stack of the upper unit (i) and the lower unit (ii) at the margin of the fan (**d**), and curvilinear bedding structures in unit (ii) beneath unit (i) (**e**). On the crater floor, a coherent capping unit (iv) and sand (v) cover bright materials (iii) (**f**). Scale bars for **c**–**f** are 50 m.

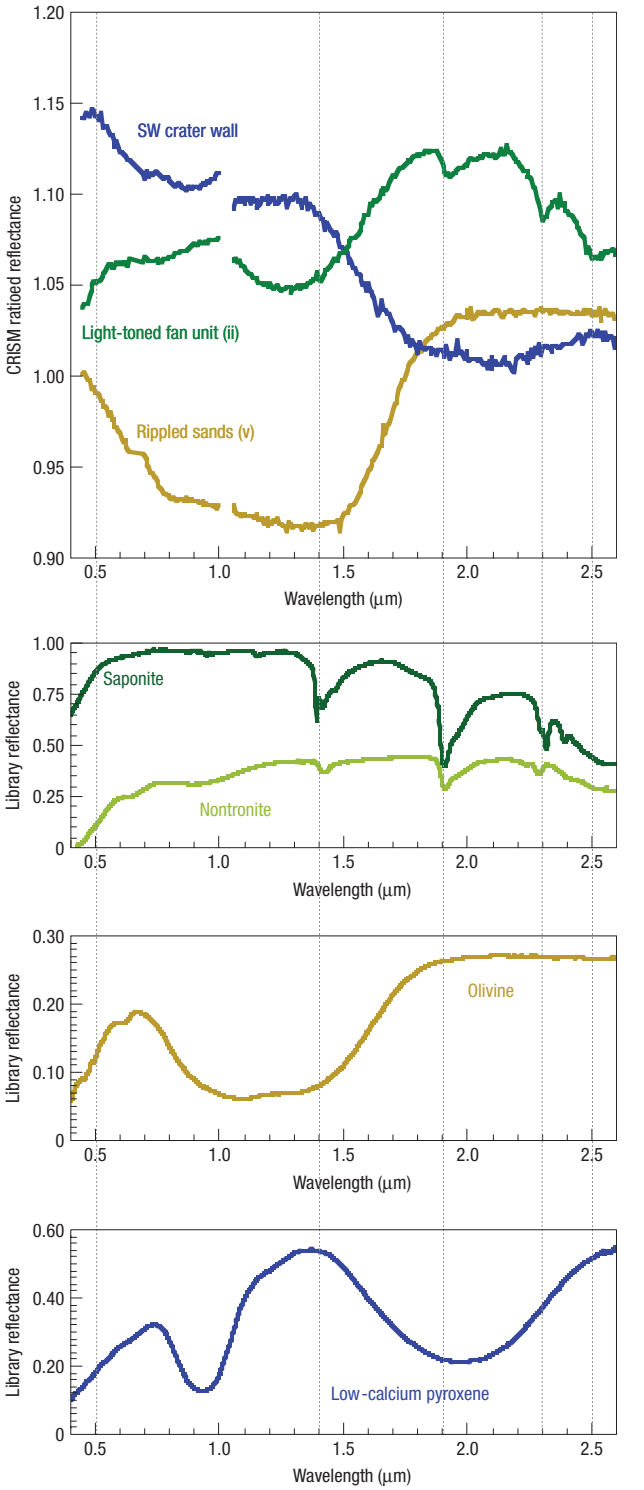

Figure 3 CRISM spectra compared with library[9] mineral reflectance spectra. CRISM 9 × 9 pixel spectra are ratioed to relatively spectrally featureless materials on the uppermost crater surface (unit iv) to highlight spectral differences and remove atmospheric and calibration artifacts (ref. 10; for unratioed spectra see Supplementary Information, Fig. S1). Colours of CRISM spectra correspond to surface colours in Fig. 2. Spectra from bright materials on the crater floor (unit iii) are similar to those in the fan (unit ii). Library spectra providing best matches to CRISM spectra are olivine (fayalite), low-calcium pyroxene (enstatite) and Fe–Mg smectites (nontronite, saponite).

smectite-rich materials and deposited smectite-rich sediments within the crater. The spectral and compositional match between iron–magnesium smectite clays within the watershed and within the crater points to a primarily allochthonous origin for the clays. This is similar to clay occurrence in terrestrial lacustrine basins because dissolved Si, Al, Fe and Mg are rarely available in proportions sufficient to precipitate complex silicates[27]. Smectites typically form under moderate to alkaline conditions[28] and have a half-life of less than a year at low pH (ref. 29), so their ubiquity within the deltaic sediments indicates that fluids were probably of moderate to alkaline pH. Thus, the fluvio-lacustrine clay deposits in Jezero crater record two periods of Martian history when the

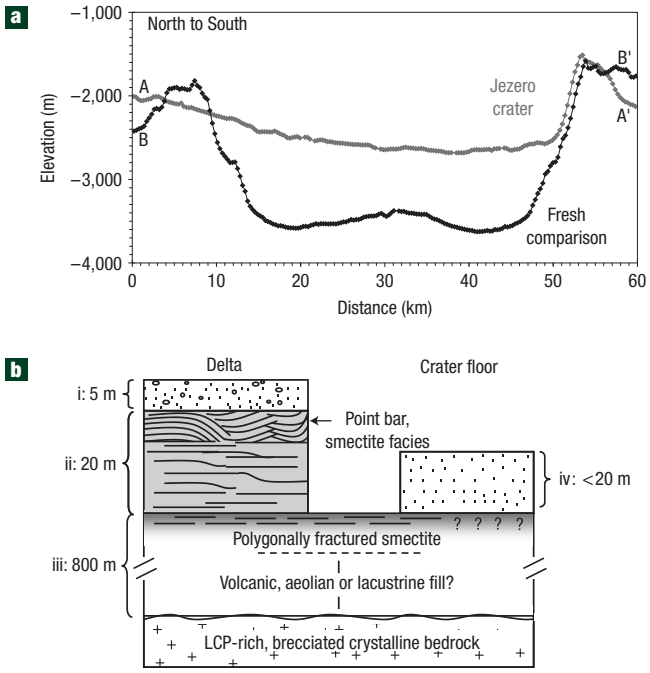

Figure 4 Topography and stratigraphy of Jezero basin. a, MOLA profile (orbit 18170 N–S) of Jezero crater and a fresh crater (125.75 E, 8.25 N) of equivalent diameter (see Supplementary Information, Fig. S2). **b**, Schematic stratigraphic column of the rock units within Jezero crater. Actual thicknesses within the units vary across the delta.

surface or near-surface was probably habitable: (1) a period of early Noachian water–rock interaction, which formed over 10^6 km^2 of iron–magnesium smectite bearing deposits in the Nili Fossae region, and (2) late Noachian to early Hesperian regional surface fluvial activity, which generated and sustained Jezero lake.

Smectite clays are notable for their ability to trap organic matter in the interlayer sites of the mineral structure. In terrestrial sedimentary basins, smectite clays are associated with many of the most organic-rich units[1]. Smectite clays and associated non-crystalline iron and aluminium oxides/hydroxides are principal binding sites of organic matter in terrestrial soils[2]. Oxidation and photochemical dissociation would rapidly destroy organic molecules exposed on the surface of Mars[30]. However, any potential organic matter transported in the Jezero crater watershed was probably buried relatively rapidly and preserved within clay-rich lacustrine and deltaic deposits. The organic-sequestering capacity of smectite-rich sediments in Jezero crater and the preservation of material from multiple habitable periods in Mars history make this crater an ideal site for future landed exploration.

Received 11 January 2008; accepted 24 April 2008; published 18 May 2008.

References

1. Kennedy, M. J., Peaver, D. R. & Hill, R. J. Mineral surface control on organic carbon in black shale. *Science* **295**, 657–660 (2002).
2. Wattel-Koekkoek, E. J. W., Buurman, P., van der Plicht, J., Wattel, E. & van Breemen, N. Mean residence time of soil organic matter associated with kaolinite and smectite. *Eur. J. Soil Sci.* **54**, 269–278 (2003).
3. Farmer, J. D. & Des Marais, D. J. Exploring for a record of ancient Martian life. *J. Geophys. Res.* **104**, 26977–26995 (1999).
4. Bibring, J.-P. *et al.* Mars surface diversity as revealed by the OMEGA/Mars Express observations. *Science* **307**, 1576–1581 (2005).
5. Poulet, F. *et al.* Phyllosilicates on Mars and implications for early martian climate. *Nature* **438**, 623–627 (2005).
6. Carr, M. *Water on Mars* 229p (Oxford Univ. Press, New York, 1996).
7. Malin, M. C. & Edgett, K. S. Evidence for persistent flow and aqueous sedimentation on early Mars. *Science* **302**, doi:10.1126/science.1090544 (2003).
8. Irwin, R. P., Howard, A., Craddock, R. & Moore, J. M. An intense terminal epoch of widespread fluvial activity on early Mars: 2. Increased runoff and paleolake development. *J. Geophys. Res.* **110**, E12S15 (2005).
9. Murchie, S. *et al.* Compact Reconnaissance Imaging Spectrometer for Mars (CRISM) on Mars Reconnaissance Orbiter (MRO). *J. Geophys. Res.* **112**, E05S03 (2007).
10. Mustard, J. F. *et al.* Hydrated silicate minerals on Mars observed by the CRISM instrument on MRO. *Nature* (submitted).
11. Moore, J. M., Howard, A., Dietrich, W. E. & Schnek, P. M. Martian layered fluvial deposits: Implications for Noachian climate scenarios. *Geophys. Res. Lett.* **30**, doi:10.1029/2003GL019002 (2003).
12. Milliken, R. E. *et al. Seventh Int. Conf. on Mars, July 9–13, 2007, Pasadena, California*, abstract 3282 (2007).
13. Grant, J. A. *et al.* HiRISE imaging of impact megabreccia and sub-meter aqueous strata in Holden Crater Mars. *Geology* **36**, 195–198 (2008).
14. Fassett, C. I. & Head, J. W. Fluvial sedimentary deposits on Mars: ancient deltas in a crater lake in the Nili Fossae region. *Geophys. Res. Lett.* **32**, L14201 (2005).
15. McEwen, A. S. *et al.* Mars Reconnaissance Orbiter's High Resolution Imaging Science Experiment (HiRISE). *J. Geophys. Res.* **112**, E05S02 (2007).
16. Greeley, R. & Guest, J. E. Geologic map of the eastern equatorial region of Mars. I-1802-B (US Geological Survey, 1987).
17. Mustard, J. F. *et al.* Olivine and pyroxene diversity in the crust of Mars. *Science* **307**, 1594–1597 (2005).
18. Hoefen, T. M. *et al.* Discovery of olivine in the Nili Fossae Region of Mars. *Science* **302**, 627–630 (2003).
19. Hamilton, V. E. & Christensen, P. R. Evidence for extensive, olivine-rich bedrock on Mars. *Geology* **33**, 433–436 (2005).
20. Mangold, N. *et al.* Mineralogy of the Nili Fossae region with OMEGA/Mars Express data: 2. Aqueous alteration of the crust. *J. Geophys. Res* **112**, E08S04 (2007).
21. Kanner, L. C., Mustard, J. F. & Gendrin, A. Assessing the limits of the Modified Gaussian Model for remote spectroscopic studies of pyroxenes on Mars. *Icarus* **187**, 442–456 (2007).
22. Bishop, J. L., Pieters, C. M. & Edwards, J. O. Infrared spectroscopic analyses on the nature of water in montmorillonite. *Clays and Clay Minerals* **42**, 702–716 (1994).
23. Swayze, G. A. *et al.* in *Proc. 11th JPL Airborne Earth Science Workshop* (ed. Green, R. O.) 373–387 (JPL Publication 03–4, Pasadena, California, 2002).
24. Nanson, G. C. Point bar and flood-plain formation of the meandering Beatton River north-eastern British Colombia, Canada. *Sedimentology* **27**, 3–29 (1980).
25. Mossop, G. D. & Flach, P. D. Deep channel sedimentation in the Lower Cretaceous McMurray Formation, Athabasca Oil Sands, Alberta. *Sedimentology* **30**, 493–509 (1983).
26. Garvin, J. B., Sakimoto, S. E. H. & Frawley, J. J. *Sixth Int. Conf. on Mars, July 20–25, 2003, Pasadena, California*, abstract 3277 (2003).
27. Chamley, H. *Clay Sedimentology* 623p (Springer, Berlin, 1989).
28. Chevrier, V., Poulet, F. & Bibring, J.-P. Early geochemical environment of Mars as determined from thermodynamics of phyllosilicates. *Nature* **448**, 60–63 (2007).
29. Huertas, F. J., Caballero, E., Jiménez de Cisneros, C., Huertas, F. & Linares, J. Kinetics of montmorillonite dissolution in granitic solutions. *Appl. Geochem.* **16**, 397–407 (2001).
30. Klein, H. P. The Viking Mission and the search for life on Mars. *Rev. Geophys.* **17**, 1655–1662 (1979).

Supplementary Information accompanies this paper on www.nature.com/naturegeoscience.

Acknowledgements

Special thanks go to the entire MRO team: without their ongoing efforts, these new discoveries would not be possible. We especially recognize the efforts of the CTX and HiRISE teams for coordinated observations with CRISM. Special thanks to Gregg Swayze for numerous discussions on interpreting CRISM spectra from the Nili Fossae region. The comments of reviewers Vincent Chevrier and Victor Baker helped improve this manuscript.

Author information

Reprints and permission information is available online at http://npg.nature.com/reprintsandpermissions. Correspondence and requests for materials should be addressed to B.L.E.